



A label-free continuous total-internal-reflection-fluorescence-based immunosensor

Henrik A. Engström^a, Per Ola Andersson^b, Sten Ohlson^{a,*}

^a Department of Chemistry and Biomedical Sciences, University of Kalmar, SE-391 82 Kalmar, Sweden

^b Division of NBC-Defence, Swedish Defence Research Agency, SE-901 82 Umeå, Sweden

Received 24 November 2005

Abstract

In this study, we continuously monitored, second-by-second, concentration changes of two different carbohydrates (maltose and panose) by using monoclonal antibodies in an optical immunosensor based on total internal reflection fluorescence. Earlier studies have demonstrated that these antibodies increase their intrinsic tryptophan fluorescence upon binding of carbohydrate antigens. Using the four immobilized monoclonal antibodies with low affinities ($K_d > 10^{-6}$ M), fast kinetics ($k_{off} > 1 \text{ s}^{-1}$), and high reversibility gave opportunities for developing a continuous immunosensor without any need for regeneration. Since intrinsic fluorescence was used, no extrinsic labeling was necessary. Sensitivity was in the range of 1–5 μM for panose, and 10–15 μM for maltose and the loss of intensity was as low as 3.5% per hour during measurements. Calculations of ΔH° and ΔS° from the temperature dependence of K_d indicated an enthalpic driven antigen–antibody binding event that is diminished upon antibody immobilization. We feel certain that weakly interacting antibodies can be used in future applications for continuous monitoring where there is a need to achieve instantaneous information on the concentration of an analyte.

© 2006 Elsevier Inc. All rights reserved.

Keywords: Biosensor; Carbohydrate; Evanescent wave; Fluorescence spectroscopy; Hapten; Immunosensor; Monoclonal antibody; Optical biosensor; Protein–carbohydrate interactions; Total internal reflection fluorescence; Transient binding; Weak affinity

Affinity-based biosensors are used to measure binding events using biological molecules such as antibodies, receptors, enzymes, or nucleic acids interfaced to a signal transducer [1]. Popular affinity-based ligands are antibodies and the resulting sensor is known as an immunosensor [2]. They can be categorized based on the detection principle, e.g., electrochemical [3] and optical [4] immunosensors. Commonly optical immunosensors utilize the evanescent wave to form the sensing device and different transducers can be used for creating an optical change, e.g., grating couplers

[5], resonant mirror [6], surface plasmon resonance (SPR) [7], interferometry [8], reflectometric interference spectroscopy [9], ellipsometry [10], and total internal reflection fluorescence (TIRF) [11]. The specific binding in all these optical immunosensors is typically characterized by high affinity (dissociation constant (K_d) $< 10^{-6}$ M) with slow off rates. The analysis is based on end-point determinations where the biosensor surface has to be regenerated to start a new measurement cycle. Assays can be very specific and sensitive enough to detect for example trace components in

* Corresponding author. Fax: +46 480 446262.

E-mail address: sten.ohlson@hik.se (S. Ohlson).

¹ Abbreviations used: a.u., arbitrary unit; ΔF , change in fluorescence intensity; ΔF_{max} , maximum change in fluorescence intensity; ΔG° , standard Gibbs free energy change; GOPS, 3-glycidioxypropyltrimethoxysilane; ΔH° , standard enthalpy change; K_a , association constant (M^{-1}); K_d , dissociation constant (M); PBS, phosphate-buffered saline; R , gas constant (8.314 J/mol · K); r^2 , correlation coefficient from linear regression; R^2 , correlation coefficient from nonlinear regression; SPR, surface plasmon resonance; ΔS° , standard entropy change; T , temperature (K); TIRF, total internal reflection fluorescence; CDR, complementary-determining region.

water samples [11]. Selection of conditions for regeneration of binding sites in high-affinity systems has to be performed carefully, since gentle elution can retain bound molecules and harsh regeneration can damage the immobilized antibody. However, by using weaker or transient binding ($K_d > 10^{-6}$ M) as the basis for recognition in the biosensor, it should be possible to monitor the analyte concentration continuously without the need for regeneration. Specificity can in fact be maintained at lower affinity if ligands are properly designed and occasionally even higher specificity can be achieved at lower affinities [12].

Earlier studies in our laboratory using weak-affinity antibodies have demonstrated their usefulness for separation in chromatography [13] and electrophoresis [14]. Attempts have been made to develop immunosensors based on these dynamic antibodies [15]. Due to the transient binding between antibody and hapten, the target can be monitored continuously second by second in a SPR-based biosensor without the need for regeneration. These antibodies showed high reversibility with affinities close to the millimolar range. Recently we showed that these antibodies increased their intrinsic fluorescence upon binding of carbohydrate haptens [16] and therefore they can possibly be used for continuous monitoring without labeling of binding partner. It has been well known for a long time that at least anticarbohydrate antibodies can change their fluorescence upon binding of haptens [17]. Immunosensors based on TIRF have received considerable attention in recent years [18–20] due to their reproducibility, precision, and robustness. The technique is based on utilization of the evanescent wave of an electromagnetic field, which extends out from the interface of two different media into the medium with lower refractive index. This field is created when light from a specific angle is totally reflected due to differences in refractive index in these two different media, e.g., quartz and water. This evanescent wave allows quantitative measurements of adsorbed molecules on the surface without any influence of any moderate bulk concentration of the same analyte.

In this study, we evaluated the potential of the TIRF technique to continuously monitor carbohydrate haptens with an immunosensor based on weakly interacting monoclonal antibodies. Of special interest was the possibility of using no labels of either antibody or hapten.

Materials and methods

Chemicals and antibodies

Maltose (Glc α 1-4Glc), cellobiose (Glc β 1-4Glc), panose (Glc α 1-6Glc α 1-4Glc), and polyclonal mouse IgG were all obtained from Sigma–Aldrich (St. Louis, MO, USA). The monoclonal mouse antibodies 38.3 (IgG3), 39.4 (IgG2b), 39.5 (IgG2b), 61.1 (IgG3), and 33C7 (IgG1) were isolated from cell culture supernatants of hybridoma cells. Purification of monoclonal antibodies was performed on a Protein A Sepharose CL 4B column (GE Health Care, Uppsala, Sweden) according to the manufacturer's instructions.

Monoclonal antibody 33C7 (IgG1) against a peptide sequence on creatine kinase MB2 (kindly provided by Lisa Leickt, University of Kalmar, Sweden) and polyclonal mouse IgG (Sigma–Aldrich) were used as nonrelevant antibodies against studied carbohydrate antigens. All other chemicals were provided by commercial sources.

Antibody coupling to TIRF slides

TIRF slides of $40 \times 30 \times 1$ mm UV quartz (BioElectroSpec, Hummelstown, PA, USA) were cleaned for 20 min at 70 °C in chromic acid, followed by an extra cleaning procedure of 1 M NaOH for 1 h at 20 °C and 0.1 M HCl for 1 h at 80 °C. Silanization was achieved by immersing the slides in 10% 3-glycidoxypropyltrimethoxysilane (GOPS) (ABCR, Karlsruhe, Germany) with 1% acetic acid. The slides were then treated with 0.05 M HCl for 2 h at 55 °C to open the epoxy ring to diol–silica. The diol–silica was oxidized to aldehyde–silica with H_2IO_6 (440 mM) for 3 h at 20 °C. The antibodies were coupled to one side of the TIRF slides by reductive amination. All antibodies were diluted in PBS (10 mM sodium phosphate, 0.15 M NaCl, pH 7.3) to a concentration of 200 μ g/ml. Sodium cyanoborohydride (80 mM) was used as a reducing agent, giving antibody coupling to aldehyde–silica by secondary amine linkage. Coupling of antibodies was performed at room temperature (21 °C) for 24 h and maintained at 6 °C for a period of 4 weeks until being used. Slides were washed with PBS before assembly of the TIRF flow cell and further analysis.

TIRF instrumentation

A spectrofluorometer (Fluorolog 3-22; Jobin Yvon, Edison, NJ, USA) complemented with a TIRF Flow System (BioElectroSpec) was used with DataMax software (version 2.10, Jobin Yvon) for collecting data. A thermostatic circulator was connected to the back block of the TIRF flow cell and the actual temperature was measured continuously using a bead probe (80PK-1, Fluke, Everett, WA, USA) with an accuracy of ± 0.3 °C. The TIRF flow cell with the different TIRF slides was assembled according to the manufacturer's instructions. Gasket thickness was 80 μ m, giving a flow cell with a surface of 3.4 cm² and a volume of 27 μ l. Syringe pump 50300 (Kloehn, Las Vegas, NV, USA) with a 5-ml syringe was used to distribute a controlled flow of 250 μ l/min to the flow cell. Excitation wavelength was 295 nm and emission intensity was measured at 345 nm with corrections for intensity fluctuations in the 450-W xenon lamp. Time scans were obtained with increment of 10 s and integration time of 1 s. To avoid photobleaching of the immobilized antibodies, excitation slit was set to correspond to a spectral bandwidth of 1 nm and was closed between integration of data points. Emission slit was set to a 10-nm spectral bandwidth. Emission spectra of immobilized antibodies were acquired with 1-nm excitation bandwidth and 5-nm

emission bandwidth, with increment of 1 nm and integration time of 0.5 s.

TIRF procedures

The TIRF slides with immobilized antibodies were evaluated by injection of at least 10 different concentrations of panose (0–800 μ M), maltose (0–8 mM), and cellobiose (0–8 mM) in PBS. Injection time was 3 min (750 μ l) and data collection was started after 30 s to ensure equilibrium and a uniform profile of each carbohydrate concentration in the flow cell. The response was measured during 2.5 min, giving 15 data points for each injection. Stock solutions of the carbohydrates were prepared in advance to ensure equilibrium between anomeric forms. Temperature was set to 25.0 $^{\circ}$ C for all experiments except for the temperature study (5.0–40.0 $^{\circ}$ C). Nonrelevant monoclonal antibody 33C7 and polyclonal mouse IgG were used to check for nonspecific intensity change of fluorescence. A blank TIRF slide with no coupled protein was also included.

TIRF data

Data for each carbohydrate injection were corrected for drifting baseline and the response was normalized for the maximum change in fluorescence (e.g., 8 mM maltose), giving a normalized response in the range of 0–100 arbitrary units (a.u.). Dissociation constants (K_d) or association constants (K_a) between antibody and carbohydrate were calculated from nonlinear regression of saturation binding curves for each antibody–antigen complex by analysis with Prism version 3.03 (GraphPad Software, San Diego, CA, USA). Data points from at least two injections of each carbohydrate concentration were averaged and a Langmuir isotherm was assumed with least square fit.

Thermodynamic study of immobilized monoclonal antibody 39.5 with maltose, in the range of 5.0–40.0 $^{\circ}$ C, was analyzed by using van't Hoff plot ($\ln K_a$ versus $1/T$), where K_a at each temperature were plotted with standard error of the mean and the linear regression was calculated with a standard error.

Results and discussion

Characteristics of TIRF-based immunosensor

As only tryptophans in proteins are excited at 295 nm, it is possible to use intrinsic fluorescence to monitor microenvironmental changes for tryptophan. The monoclonal antibody 39.5 carries two tryptophans in the complementary-determining regions (CDRs) with another four tryptophans in close proximity to these regions (unpublished data). One of the tryptophans is located in CDR 3 of the light chain and one in CDR 1 of the heavy chain. When tryptophan is found in the CDRs, these aromatic residues are frequently found to be involved in the interaction with antigen [21] because of their hydrophobic effects [22].

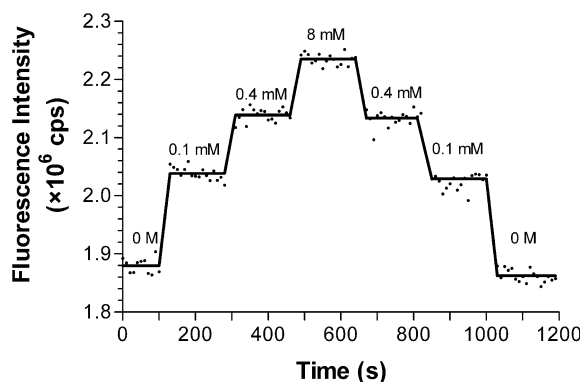


Fig. 1. Intensity response of the intrinsic fluorescence of the 39.5 antibody upon interaction with maltose. The intrinsic fluorescence is changed with step wise injections of different concentrations of maltose (0, 0.1, 0.4, and 8 mM). Lines represent mean value of data points for each maltose injection at 25 $^{\circ}$ C.

In accordance with free antibody 39.5 [16] an intensity enhancement of intrinsic fluorescence was seen for the immobilized 39.5 (Fig. 1) and for its sister antibodies 38.3, 39.4, and 61.1 (Fig. 2) upon interaction with the carbohydrate antigens maltose and panose but not with cellobiose which is a similar nonbinding carbohydrate (Figs. 1 and 2). Immobilization of all antibodies to the different TIRF surfaces was successful due to the appearance of a protein fluorescence signal, as compared with no signal from the blank surface. A certain loss of activity of antibodies is expected after immobilization onto the slide surface. We have earlier noticed for the antibody 39.5 a loss of approximately 50% of the activity when immobilized onto a silica surface [13]. A small decrease in fluorescence intensity was observed over time during operation. Immobilized 39.5 demonstrated the highest stability with a decrease of 3.5% per hour, which is barely seen in Fig. 1, whereas the other antibodies were in the range of 7–8% per hour. Drift of baseline was probably caused by a combination of photobleaching and antibody leakage and/or denaturation from the surface of the TIRF slide. Specificity of the immunosensor was further confirmed by using identical carbohydrate antigens with irrelevant monoclonal antibody 33C7 (IgG1), polyclonal mouse IgG, or a blank TIRF surface without antibodies (Fig. 3). The difference in geometrical structure in maltose (Glc α 1–4Glc) and cellobiose (Glc β 1–4Glc) results apparently in a binding in the paratope for maltose and therefore a closer proximity to tryptophan residues in, or adjacent to, the binding cavity. Interactions between tryptophan and maltose or panose are strong enough to alter the photophysical properties of tryptophan residues.

Binding data of TIRF-based immunosensor

Dissociation constants (K_d) for the antibodies were extracted from adsorption isotherms. One example is seen in Fig. 4 where monoclonal antibody 39.5 interacted with maltose. Response from carbohydrate injections was normalized to the maximum carbohydrate concentration (e.g. 8 mM for maltose) and corrected for a drifting baseline. Intensity data

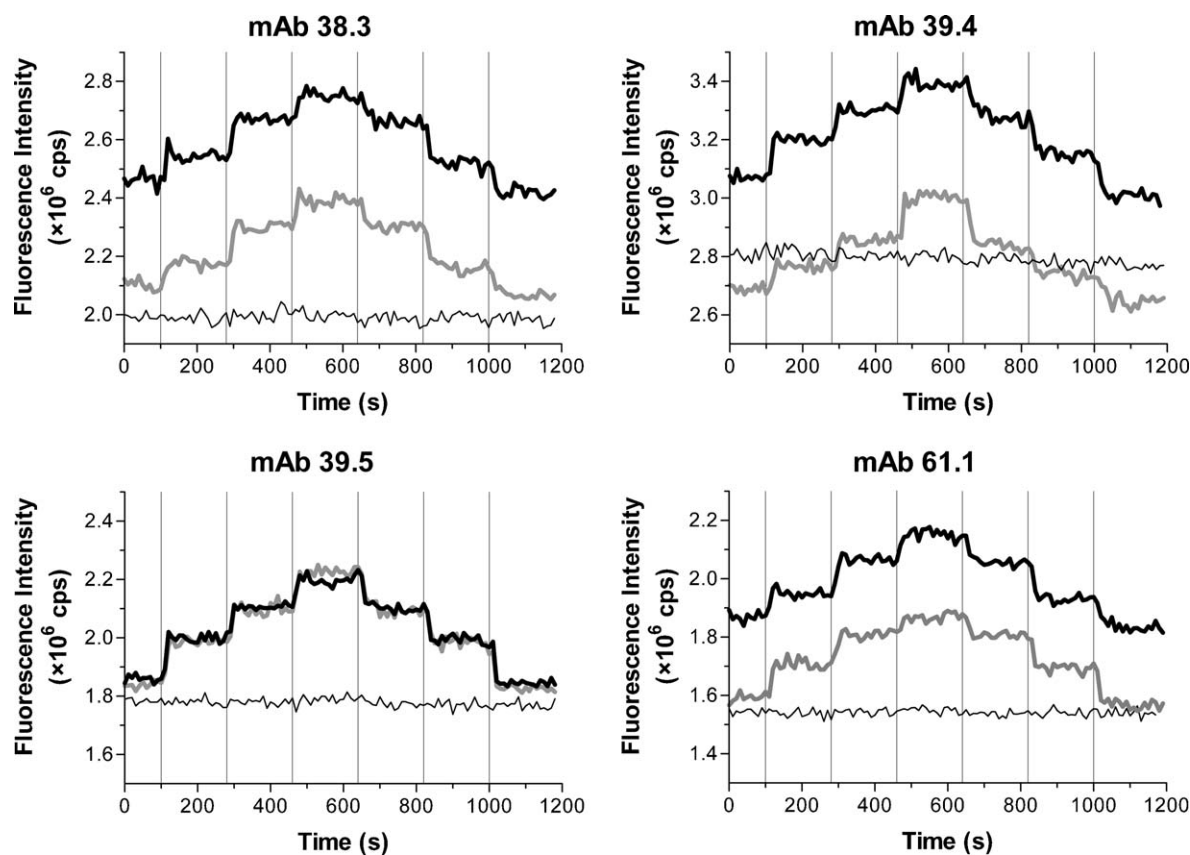


Fig. 2. Time response of the continuous TIRF-based immunosensor. Step wise injections of different concentrations of maltose (0–8 mM), panose (0–0.8 mM), and cellobiose (0–8 mM) with four different immobilized monoclonal antibodies (38.3, 39.4, 39.5, and 61.1). The vertical lines indicate the change in concentration for maltose (black line), panose (gray line), and cellobiose (thin line).

from each injection of carbohydrate (Figs. 1 and 2) give a mean value with standard deviation (for 39.5; Fig. 4). Dissociation constants for all the monoclonal antibodies against both maltose and panose are listed in Table 1. All antibodies possess higher K_d values for maltose than for panose and monoclonal antibody 39.4 has a significantly higher K_d value for panose than for the other antibodies.

In another biosensor study based on surface plasmon resonance with immobilized 39.5 antibodies on a dextran-layered chip [15], the TIRF slides showed lower affinity ($K_d = 87 \mu\text{M}$ for 39.5 maltose). This can be due to increased flexibility of the dextran layer with reduced hindering effects upon the binding of carbohydrate to the antibody. It should be noted that different buffers but the same pH were used in the studies, which can reflect differences in K_d . Immobilization of 39.5 onto TIRF slides did not affect the emission spectra. Changes in spectra with, e.g., blue or red shift are normally caused by the tryptophan being exposed in a more apolar or polar environment, respectively. This was not detected upon comparison between spectra of immobilized and free 39.5.

Thermodynamic analysis of binding to immobilized monoclonal antibody 39.5

If the standard enthalpy change (ΔH°) does not vary within the studied temperature interval of 5.0–40.0 °C,

the van't Hoff plot results in a straight line in accordance to the equation $\ln K_a = -\Delta H^\circ/RT + \Delta S^\circ/R$, where ΔS° is the standard entropy change and $R = 8.314 \text{ J/mol K}$. The linearity is clearly shown in Fig. 5 for free [16] and for immobilized 39.5 antibodies. From the slope and intercept of the y axis, ΔH° and ΔS° are calculated and given in Table 2 together with standard Gibbs energy (ΔG°) computed from $-RT \ln K_a$. With respect to a 95% confidence interval the linear regression lines are significantly separated, but the immobilization process had only a minor influence on the ΔH° and ΔS° , which will be discussed below.

Results from the temperature study of antibody 39.5 during maltose binding (Table 3) are close to those earlier determined [16], showing an association constant (K_a) characteristic with a 10-fold decrease when going from 5 to 40 °C and a recognition event that is enthalpy driven and entropic unfavorable. The obtained thermodynamic parameters are also close to other reported values on related low-affinity binding systems [23–25]. It is likely that the negative enthalpy change upon binding originates from electrostatic interactions as van der Waals forces and hydrogen bonding. Noteworthy, it is argued based on several different methods, e.g., NMR and X-ray studies (see [24] and references therein), that the aromatic amino acids in and near the paratope are essential in carbohydrate–protein binding through complex

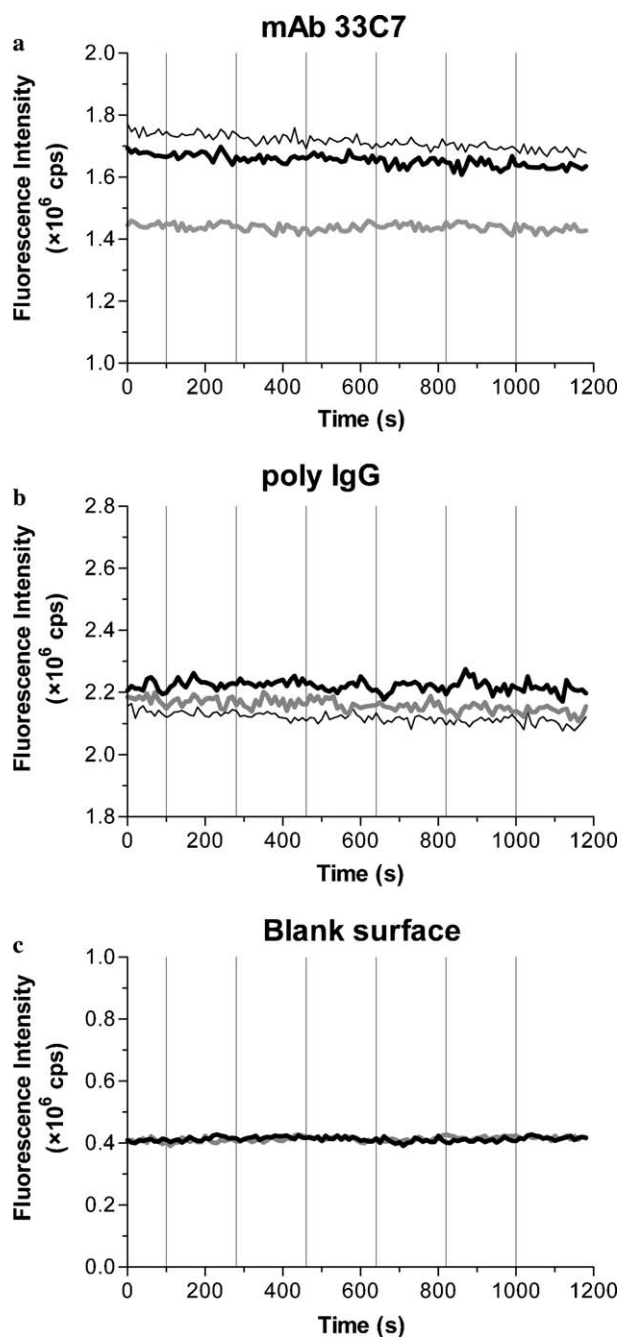


Fig. 3. Negative controls for the continuous TIRF-based immunosensor. Injections of different concentrations of maltose (0–8 mM), panose (0–0.8 mM), and cellobiose (0–8 mM) with immobilized irrelevant antibodies (a) 33C7 and (b) polyclonal IgG and (c) blank surface. The vertical lines indicate the change in concentration for maltose (black line), panose (gray line), and cellobiose (thin line).

stabilizing by CH- π stacking interactions, van der Waals contacts, and hydrogen bonding. As mentioned above, several tryptophans are in close proximity to the binding regions in antibody 39.5, and since all maltose-specific binding antibodies investigated so far by us show fluorescence enhancement upon maltose titrations (Fig. 2), it is very likely that they all possess several aromatic acids, at least tryptophans, located in a similar way.

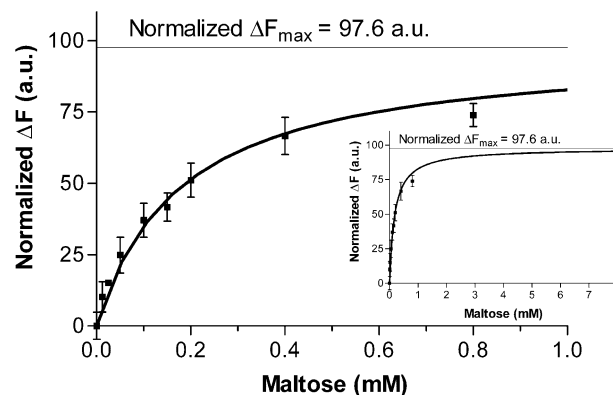


Fig. 4. Saturation binding curve of the immobilized monoclonal 39.5 antibody upon interaction with maltose at 25 °C. Error bars represent the standard deviation from at least two injections for each carbohydrate concentration. For clarity, concentrations above 1 mM maltose are shown as an inset.

Table 1
Dissociation constants (K_d) with standard error (SE) for the different immobilized monoclonal antibodies at 25.0 °C with maltose and panose

Immobilized monoclonal antibody	Maltose		Panose	
	$K_d \pm \text{SE}$ (μM)	R^2	$K_d \pm \text{SE}$ (μM)	R^2
38.3	117.7 ± 8.8	0.993	13.5 ± 1.2	0.991
39.4	175.9 ± 9.9	0.996	33.5 ± 2.7	0.994
39.5	179.7 ± 18.8	0.988	13.7 ± 0.8	0.998
61.1	127.1 ± 5.8	0.998	13.5 ± 1.1	0.993

For antibody 39.5 the affinity for both maltose and panose decreases upon immobilization of the antibodies. The K_d measured at 25 °C has increased from 81.2 to 179.7 μM for maltose and from 9.6 to 13.7 μM for panose. Thus, a substantially larger affinity loss against maltose is obtained. The reason for this can only be speculated. However, for maltose, thermodynamic parameters displayed in Table 2 might give a hint, although the standard errors of ΔH° and ΔS° are relatively high. The binding affinity reflected in a standard Gibbs energy goes from -23.35 to -21.39 kJ/mol (Table 2) due to covalent immobilization of antibody 39.5. The fundamental thermodynamic relationship $\Delta G^\circ = \Delta H^\circ - T\Delta S^\circ$ together with the data in Table 2 indicate that ΔH° changes in the same direction as ΔG° while $-T\Delta S^\circ$ slightly alters in the opposite direction to ΔG° . In other words, the lower affinity measured with immobilized antibodies are related to a lower enthalpic contribution to the binding. Thus the interaction energy has decreased in relation to antibodies free in solution. This possible distortion of electrostatic interaction upon immobilization might have been induced by several factors, e.g., steric hindrance of the antibody on the planar surface, random immobilization to amino groups of the antibody, and mass transfer effects during hapten transport to the paratope of the antibody. Differences in affinities and the enhanced ΔG° for panose relative to maltose come most likely from a favorable ΔS° , as was discussed in our earlier report [16]. This might explain the lower affinity loss

Table 2
Thermodynamic data for the interaction of maltose with immobilized monoclonal antibody 39.5 and free in solution

Antibody 39.5	ΔG° (kJ/mol)	ΔH° (kJ/mol)	ΔS° (J/mol K)
Immobilized on surface	$-(21.39 \pm 0.26)$	$-(47.13 \pm 3.19)$	$-(85.85 \pm 10.83)$
Free in solution	$-(23.35 \pm 0.14)$	$-(51.22 \pm 2.47)$	$-(93.98 \pm 8.41)$

Standard Gibbs free energy (ΔG°), standard enthalpy (ΔH°), and standard entropy (ΔS°) are shown with a standard error at 25 °C.

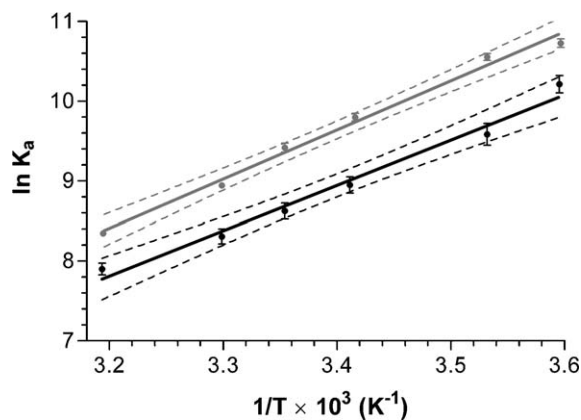


Fig. 5. van't Hoff plots for the binding of maltose with immobilized (black line, $r^2 = 0.982$) and free monoclonal 39.5 antibody in solution (gray line, $r^2 = 0.991$). Error bars represent standard error of the mean and dashed lines represent a 95% confidence interval of the linear regression.

Table 3
Dissociation constants (K_d) with standard error (SE) for the immobilized monoclonal 39.5 antibody with maltose at different temperatures

Temperature (°C)	Immobilized 39.5 antibody with maltose	
	$K_d \pm SE$ (μM)	R^2
5.0	36.6 ± 4.2	0.987
10.0	68.7 ± 10.1	0.970
20.0	129.6 ± 13.8	0.988
25.0	179.7 ± 18.8	0.988
30.0	246.4 ± 23.7	0.991
40.0	370.3 ± 28.2	0.993

between 39.5 and panose upon immobilization; i.e., the hydrophobic effect is more or less unaffected and insensitive to whether the antibody is covalently bound to a surface or is free in solution. However, more experiments have to be performed to elucidate this issue.

The continuous TIRF-based immunosensor

As seen from Figs. 1 and 2, we can follow the change of carbohydrate concentration by a concomitant fluorescence change in the form of square-like pulses. New equilibria that reflect the concentration of the analyte in every moment are quickly obtained. This truly continuous binding behavior is possible due to the weak and transient nature of antigen binding to the immobilized antibody where the binding, K_d , is in the range of 10–200 μM with expected dissociation rate constants (k_{off}) of $>1 \text{ s}^{-1}$ for, e.g., the 39.5 maltose pair at 25 °C [15,16]. The key to monitoring continuously is the favorable kinetics, especially the

high off rates of antigen from the antigen–antibody complex. Given the rapid off rates, half-lives of these complexes are short (within seconds) and mass transport effects are expected not to be rate limiting.

The sensitivity (defined as detectability at twice the variation of noise) of the transient immunosensor is dependant on the affinity of the system. For example as panose has an order of magnitude higher affinity than maltose for 39.5 (see Table 1), sensitivity was in the range of 1–5 μM for panose and 10–15 μM for maltose at 25 °C. This is much less than in a traditional immunoassay where the detection level can be in the nM range. Sensitivity can therefore be a problem for weak-affinity interactions where a correspondingly smaller fraction of analyte is bound to the antibody. However, this can be compensated by working with highly sensitive transducer platforms such as optical biosensors based on fluorescence. In this work we have used no labels and such an immunosensor based on fluorescence is easy to construct and use but has limitations for example in detectability. By using reporter molecules such as chemical fluorophores and quantum dots, it is expected that sensitivity can be significantly increased. In addition inherent fluorescence markers such as tryptophan residues of the antibody or other protein molecule have to be affected by the binding event. An advantage with the weak immunosensor can be a wider linearity range of the adsorption isotherm, where for example in these studies linear measurements were up to a few hundred μM maltose. Antibodies with affinities of mM should be valuable for continuous monitoring such as glucose measurements for diabetes control [26]. Continuous glucose monitoring, instead of a few spot measurements per day, would result in a better estimation of the correct glucose level of diabetic patients and in turn would optimize their insulin therapy.

Another major concern when dealing with transient interactions is specificity or selectivity of binding. We have discussed this issue in detail in a previous paper [16] and a major conclusion is that there is no strict correlation between affinity and specificity. Using lower affinities can indeed be more specific than the reversed situation. As shown in Figs. 2 and 3 we are experiencing high specificity versus the structural analog of cellobiose and other non-binding carbohydrates (data not shown). It is obvious that we have a completely different situation when dealing with cruder samples such as serum-based matrices. Here nonspecific interactions and background fluorescence response from present proteins can be plentiful. In this context it is important to estimate the presence of nonspecific interactions by studying the binding to blank surfaces or more

preferably to irrelevant antibodies with no appreciable affinity to studied antigens. As shown in Fig. 3, we were not able to detect any nonspecific binding to at least these antibodies.

With regard to stability of the TIRF immunosensor (see results above) we noticed a loss of activity during operation. Still we were able to use the same slide for repeated operational sessions up to 2 weeks before replacement of a new slide with immobilized antibodies. An important feature of the weak immunosensor is that no regeneration of the antibody surface was required during the analytical session which probably increased its operational stability significantly.

Conclusions

We have in this work shown that TIRF can be used to monitor weak or transient binding. Four different monoclonal antibodies with dissociation constants from a few μM to the mM range were successfully used for continuous measurement of changing antigen concentrations. Highly reversible binding makes it possible to measure changes in concentration instantly in a relatively wide span. In this case no fluorescence labeling was required since the intrinsic fluorescence from tryptophan in the paratope or adjacent to it was increased upon binding of carbohydrate antigens. A key issue to be solved for developing relevant applications is the sensitivity of the immunosensor as transient binding leads to a smaller fraction of antigen/analyte bound to antibody/receptor, thereby giving rise to lower signals. Nevertheless, by using transient interaction of weak antibodies with rapid off rates that facilitate equilibrium changes in a short time without regeneration, we can use the immunosensor in a truly continuous mode. We have also concluded, not unexpectedly, that the affinity for the antibodies is influenced, in this case decreased by immobilization, which is probably related to a lesser contribution of enthalpy to the binding. The environment of the matrix surface and the covalent linkage to the antibodies certainly affects binding behavior which has to be taken into account when designing a continuous immunosensor. This work has clearly demonstrated that a TIRF-based immunosensor based on transient binding can monitor changes in antigen concentrations instantly and is suitable for applications where instant and continuous information would be valuable in process analysis, environmental surveillance, and clinical monitoring of life-threatening situations, such as hypoglycemia [27], septic shock [28], and acute myocardial infarction [29]. Whole libraries of weak immunoglobulin reagents of not only monoclonal antibodies but also fragments such as single-chain Fv expressed by phage display should be come available.

Acknowledgments

We thank Eva Åström for information on protein sequence of the CDRs of monoclonal antibody 39.5 and

Maria Bergström for stimulating discussions. This work was supported by grants from the University of Kalmar and the Knowledge Foundation.

References

- [1] P. D'Orazio, Biosensors in clinical chemistry, *Clin. Chim. Acta* 334 (2003) 41–69.
- [2] P.B. Lippa, L.J. Sokoll, D.W. Chan, Immunosenors—principles and applications to clinical chemistry, *Clin. Chim. Acta* 314 (2001) 1–26.
- [3] A.L. Ghindilis, P. Atanasov, M. Wilkins, E. Wilkins, Immunosenors: electrochemical sensing and other engineering approaches, *Biosens. Bioelectron.* 13 (1998) 113–131.
- [4] C.L. Baird, D.G. Myszka, Current and emerging commercial optical biosensors, *J. Mol. Recognit.* 14 (2001) 261–268.
- [5] E. Ehrentreich-Förster, F.W. Scheller, F.F. Bier, Detection of progesterone in whole blood samples, *Biosens. Bioelectron.* 18 (2003) 375–380.
- [6] P. Skládal, Effect of methanol on the interaction of monoclonal antibody with free and immobilized atrazine studied using the resonant mirror-based biosensor, *Biosens. Bioelectron.* 14 (1999) 257–263.
- [7] R.J. Green, R.A. Frazier, K.M. Shakesheff, M.C. Davies, C.J. Roberts, S.J. Tendler, Surface plasmon resonance analysis of dynamic biological interactions with biomaterials, *Biomaterials* 21 (2000) 1823–1835.
- [8] F. Prieto, B. Sepúlveda, A. Calle, A. Llobera, C. Domínguez, L.M. Lechuga, Integrated Mach-Zehnder interferometer based on ARROW structures for biosensor applications, *Sensor. Actuator. B* 92 (2003) 151–158.
- [9] G. Proll, M. Kumpf, M. Mehlmann, J. Tschmelak, H. Griffith, R. Abuknesha, G. Gauglitz, Monitoring an antibody affinity chromatography with a label-free optical biosensor technique, *J. Immunol. Methods* 292 (2004) 35–42.
- [10] Y.M. Bae, B.K. Oh, W. Lee, W.H. Lee, J.W. Choi, Detection of insulin-antibody binding on a solid surface using imaging ellipsometry, *Biosens. Bioelectron.* 20 (2004) 895–902.
- [11] J. Tschmelak, N. Käppel, G. Gauglitz, TIRF-based biosensor for sensitive detection of progesterone in milk based on ultra-sensitive progesterone detection in water, *Anal. Bioanal. Chem.* 382 (2005) 1895–1903.
- [12] M.H.V. Van Regenmortel, From absolute to exquisite specificity. Reflections on the fuzzy nature of species, specificity and antigenic sites, *J. Immunol. Methods* 216 (1998) 37–48.
- [13] S. Ohlson, M. Bergström, P. Pålsson, A. Lundblad, Use of monoclonal antibodies for weak affinity chromatography, *J. Chromatogr. A* 758 (1997) 199–208.
- [14] H. Ljungberg, S. Ohlson, S. Nilsson, Exploitation of a monoclonal antibody for weak affinity-based separation in capillary gel electrophoresis, *Electrophoresis* 19 (1998) 461–464.
- [15] S. Ohlson, C. Jungar, M. Strandh, C.F. Mandenius, Continuous weak-affinity immunosensing, *Trends Biotechnol.* 18 (2000) 49–52.
- [16] H.A. Engström, P.O. Andersson, S. Ohlson, Analysis of the specificity and thermodynamics of the interaction between low affinity antibodies and carbohydrate antigens using fluorescence spectroscopy, *J. Immunol. Methods* 297 (2005) 203–211.
- [17] M.E. Jolley, C.P.J. Glaudemans, The determination of binding constants for binding between carbohydrate ligands and certain proteins, *Carbohydr. Res.* 33 (1974) 377–382.
- [18] C. Domenici, A. Schirone, M. Celebre, A. Ahluwalia, D. De Rossi, Development of a TIRF immunosensor: modelling the equilibrium behaviour of a competitive system, *Biosens. Bioelectron.* 10 (1995) 371–378.
- [19] A. Akkoyun, U. Bilitewski, Optimisation of glass surfaces for optical immunosenors, *Biosens. Bioelectron.* 17 (2002) 655–664.
- [20] J. Tschmelak, G. Proll, G. Gauglitz, Verification of performance with the automated direct optical TIRF immunosensor (River Analyser) in single and multi-analyte assays with real water samples, *Biosens. Bioelectron.* 20 (2004) 743–752.
- [21] E.A. Padlan, Anatomy of the antibody molecule, *Mol. Immunol.* 31 (1994) 169–217.

- [22] M. Levitt, M.F. Perutz, Aromatic rings act as hydrogen bond acceptors, *J. Mol. Biol.* 201 (1988) 751–754.
- [23] E.M. Nashed, C.P.J. Glaudemans, Observations on the binding of four anti-carbohydrate monoclonal antibodies to their homologous ligands, *J. Biol. Chem.* 271 (1996) 8209–8214.
- [24] J.L. Asensio, F.J. Cañada, H.C. Siebert, J. Laynez, A. Poveda, P.M. Nieto, U.M. Soedjanaamadja, H.J. Gabius, J. Jiménez-Barbero, Structural basis for chitin recognition by defense proteins: GlcNAc residues are bound in a multivalent fashion by extended binding sites in hevein domains, *Chem. Biol.* 7 (2000) 529–543.
- [25] A. Lammerts van Bueren, A.B. Boraston, Binding sub-site dissection of a carbohydrate-binding module reveals the contribution of entropy to oligosaccharide recognition at “non-primary” binding subsites, *J. Mol. Biol.* 340 (2004) 869–879.
- [26] C. Valeri, P. Pozzilli, D. Leslie, Glucose control in diabetes, *Diab. Metab. Res. Rev.* 20 (Suppl. 2) (2004) S1–S8.
- [27] T. Koschinsky, L. Heinemann, Sensors for glucose monitoring: technical and clinical aspects, *Diabetes/Metabolism Res. Rev.* 17 (2001) 113–123.
- [28] D. Annane, E. Bellissant, J.-M. Cavillon, Septic shock, *Lancet* 365 (2005) 63–78.
- [29] A.H.B. Wu, A. Smith, R.H. Christenson, M.M. Murakami, F.S. Apple, Evaluation of a point-of-care assay for cardiac markers for patients suspected of acute myocardial infarction, *Clin. Chim. Acta* 346 (2004) 211–219.